Reprinted from **Applied Optics,** Vol. 19, page 1921, June 15, 1980

Infrared reflectance spectroscopy and thermographic investigations of the Shroud of Turin

J. S. Accetta and J. Stephen Baumgart

In this paper we present the results of the IR investigations of the controversial Turin Shroud. Reflectance spectroscopy in the 3–5- and 8–14-μm bands was attempted *in situ* using commercial equipment with moderate success. Spectral comparisons are made between laboratory reflectance data and selected Shroud features. Infrared thermographic imaging was accomplished with an enhanced contrast technique using external illumination. Due to the spectral similarities of most features observed, we show that the results are inconclusive. The IR imagery yielded results that are consistent with expectations with no anomalies observed.

I. Background

Rarely in the course of routine nondestructive testing does the opportunity arise to apply established techniques to archeological relics, especially one as controversial as the Turin Shroud. This ancient piece of linen (authenticated to ~1350 A.D.) bears the frontal and dorsal images of a man replete with the classical marks of crucifixion.[1] The medium of presentation appears to be nearly singular with very few parallels in the history of renaissance art[2] and has recently undergone a series of nondestructive tests to determine the physical characteristics of the image.

Although the Shroud has been examined on several occasions in the past, a comprehensive data base upon which to do hypothesis testing does not exist. That such a data base might be established became the objective of a number of interested scientists from the international community several years ago and came to fruition in 5 days of testing in Turin, Italy in October 1978. It was not clear *a priori* which specific techniques might be most useful in decoding the Shroud. Accordingly, the philosophy to employ as many nondestructive tests as possible was adopted early. Two of the suggested techniques involved the IR spectral reflectance of several selected features of cloth and IR wide-field imagery. The rationale was to attempt to glean some information on the chemistry of selected features from spectroscopic data. In addition the imagery might yield details not apparent in the visible region of the spectrum.

Regardless of the religious implications of the image, the physical characteristics of the cloth are subject to classical experimental techniques. The effort provided a rather challenging situation in the context of using readily available equipment, with limited budgets, on a single opportunity basis.

This paper is divided into two parts. The first (Sec. II) discusses the technique and results of the IR reflectance spectroscopy effort, and the other part (Sec. III) is concerned with the results of the imaging attempts in the 8–14- and 3–5-μm bands.

II. Infrared Reflectance Spectroscopy

A. Introduction

Consistent with the requirement of using readily available equipment, the IR bands most amenable to investigation are the 3–5- and 8–14-μm regions where readily available detectors and atmospheric windows conveniently coexist. Furthermore, simplicity demanded that the single-beam mode of spectroscopy be employed. This configuration consisted of alternately measuring the sample and a reflectance standard in identical geometries. In spite of the notorious difficulties associated with this mode due to short term variations in atmospheric absorption,[3] circumstances dictated no other alternative.

J. S. Accetta is with Lockheed Missiles & Space Company, Inc., Albuquerque, New Mexico 87111, and J. S. Baumgart is with EG&G Corporation, Los Alamos, New Mexico 87545.

Received 31 March 1980.
0003-6935/80/121921-09$00.50/0.

B. Theory of the Measurement

Consider a generalized radiometer with collecting optics and a wavelength selection device. An externally illuminated sample with spectral reflectance $\rho(\lambda)$ is within the FOV. The output voltage V_s from the radiometer as a function of wavelength can be described as a convolution integral:

$$V_s(\lambda) = K \int_0^\infty \rho_s(\lambda')L(\lambda')S(\lambda' - \lambda)d\lambda', \quad (1)$$

where K = constant of proportionality describing the geometry;
$L(\lambda)$ = spectral radiance of the source;
$\rho_s(\lambda)$ = spectral reflectivity of the sample; and
$S(\lambda)$ = spectral response of the radiometer.

The voltage output at each λ is an integral over the spectral response function $S(\lambda)$ of the filter element. If $S(\lambda)$ is sufficiently narrow, i.e., approaches a spectrally weighted δ function, $R(\lambda')\delta(\lambda' - \lambda)$, the integral vanishes yielding

$$V_s(\lambda) \simeq K\rho_s(\lambda)L(\lambda)R(\lambda). \quad (2)$$

The procedure is justified if $\lambda/(\Delta\lambda) \gg 1$, where $\Delta\lambda$ is the approximate spectral bandpass of the device. For the instrument used in the experiment $\lambda/(\Delta\lambda) \simeq 60$.

If a reference standard with spectral reflectance $\rho_R(\lambda)$ is observed, by the approximation described above, the voltage V_R output of the radiometer can also be written as

$$V_R(\lambda) \simeq K\rho_R(\lambda)L(\lambda)R(\lambda). \quad (3)$$

The ratio of the two approximations from Eqs. (2) and (3) yields

$$\rho_S(\lambda) \simeq \frac{V_S(\lambda)}{V_R(\lambda)}\rho_R(\lambda) \quad (4)$$

as the final expression relating the spectral reflectance of the unknown sample to the known output voltages and the known spectral reflectance of the standard.

The assumption implicit in the above derivations is that both the reference standard and sample have nearly identical geometrical reflectance distributions and that neither exhibits any dependence on temperature. A further requirement is that the self-emission component and reflected background radiation be eliminated from the measurement. The extent to which these requirements were satisfied is discussed in the following text.

C. Experimental Configuration

The experimental configuration is shown in Fig. 1. The radiometer was a Barnes model 12-550 with 11-cm collecting optics and 2.5-mrad FOV. This instrument is equipped with a HgCdTe detector and a two-segment circular variable filter operating in the 3–5- and 8–14-μm bands with a spectral resolution of $\lambda/(\Delta\lambda) \simeq 60$. Nominal scanning time for each band was 15 sec. The blackbody source was operated at 980°C and focused with a set of $f/1$ NaCl lenses to a spot diameter of ~2 cm on the target. Although the hydroscopic nature of these lenses was a source of some difficulty, both the transparency in the visible region and relative low cost rendered the choice most suitable for this application. The incident flux from the blackbody source resulted in an equilibrium cloth surface temperature of 59°C (138°F).

For the rejection of the background and self-emission components, the source was chopped at 500 Hz and processed with a synchronous amplifier. This procedure yielded a measured ac to dc component rejection ratio of 50:1. A minicomputer was programmed to automate data recording. However, a failure early in the experiment necessitated strip chart recording, and as a consequence the advantage of real-time signal averaging was lost. This became a major source of difficulty because of the poor SNR encountered from inherent low reflectance (5–10%) of the cloth and atmospheric fluctuations that on occasion exceeded ±20% of the average signal levels. Transmission of the cloth was estimated at 10% and was not considered a significant effect.

Because cloth is quite diffuse in reflectance, exhibiting a nearly Lambertian distribution, it was necessary by the approximation set forth above to use a reflectance standard with comparable distribution.

Gold-plated sandpaper of 240 grit is an excellent choice for this application.[3] However to preclude changing attenuator settings when alternating between sample and standard it was advantageous to choose a standard whose absolute reflectance is within a factor of 2 or so of the absolute value of the sample. Flat black enamel sprayed on 240-grit sandpaper was found to reasonably satisfy this requirement. Laboratory measurement of the standard revealed Lambertian behavior out to 30° of the surface normal. An advantage of this diffuse behavior is the relative insensitivity to geometry when the standard is inserted in the target plane.

The spectral resolution available with this instrument was demonstrated by example. With the configuration shown in Fig. 1, using a gold standard as the target, a sample of polyethelene was interposed between the target and the radiometer. The absorption spectra obtained are shown in Fig. 2 and compared with the absorption spectra of the same sample of polyethelene

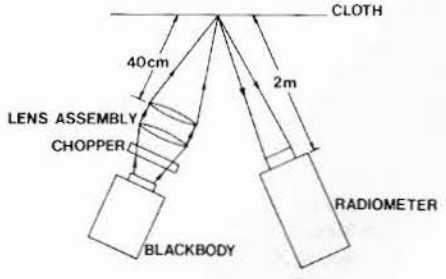

Fig. 1. Experimental configuration of reflectance spectroscopy measurement.

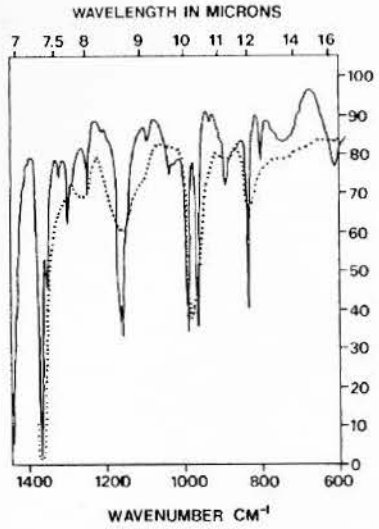

Fig. 2. Spectral resolution comparisons between a moderate resolution laboratory instrument and experimental setup (dotted curve) using polyethylene as a sample (8–14 μm).

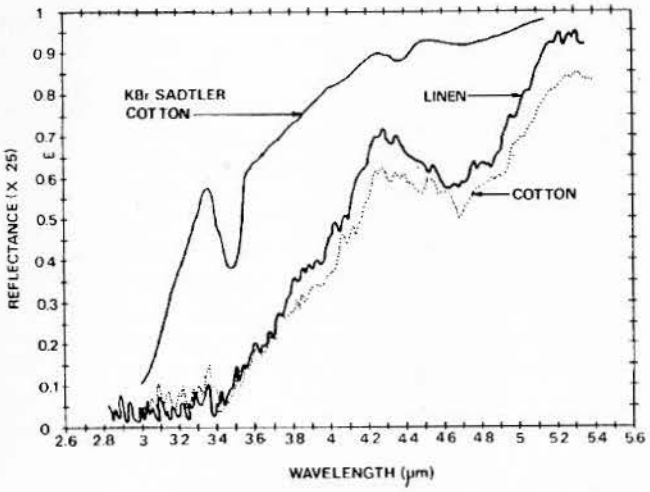

Fig. 3. Absolute spectral reflectance of linen and cotton in 3–5-μm band. Sadtler standard cotton in transmission is also shown for comparison.

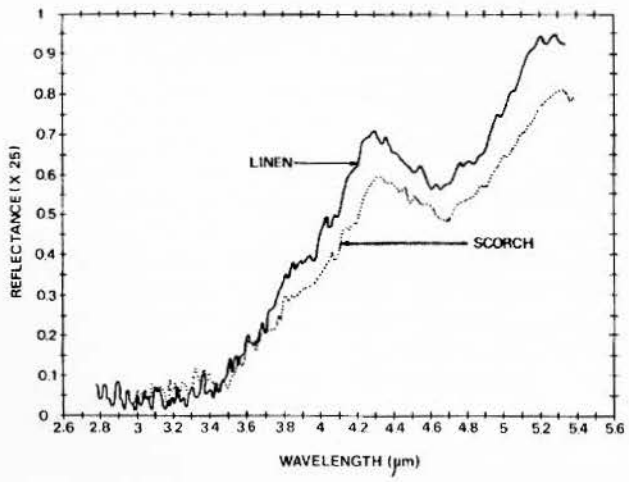

Fig. 4. Absolute spectral reflectance comparison of linen and scorched linen in 3–5-μm band.

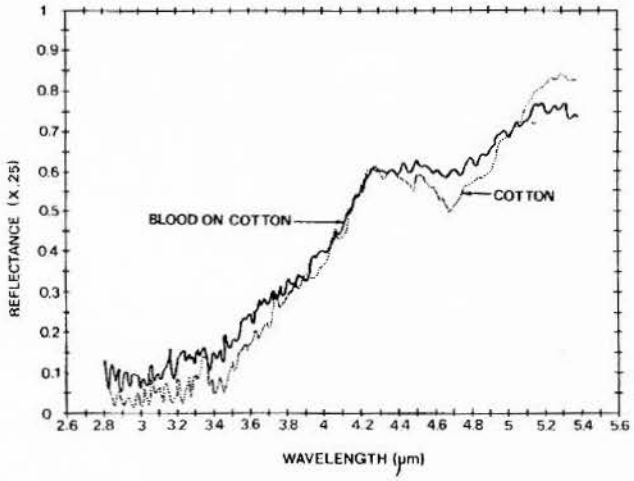

Fig. 5. Absolute spectral reflectance comparisons of cotton and whole blood-on-cotton in 3–5-μm band.

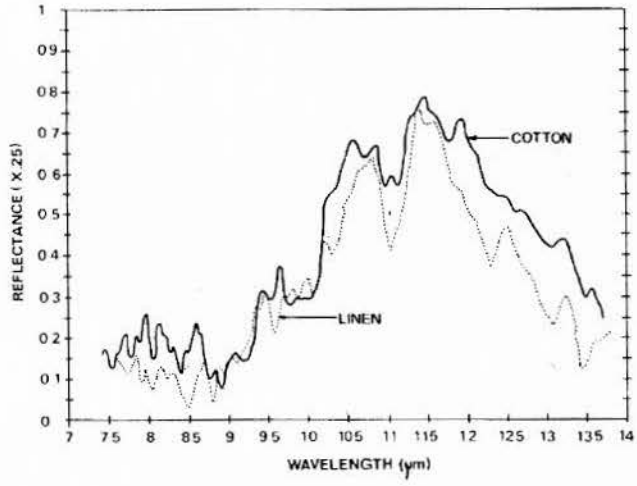

Fig. 6. Absolute spectral reflectance comparisons of linen and cotton in 8–14-μm band.

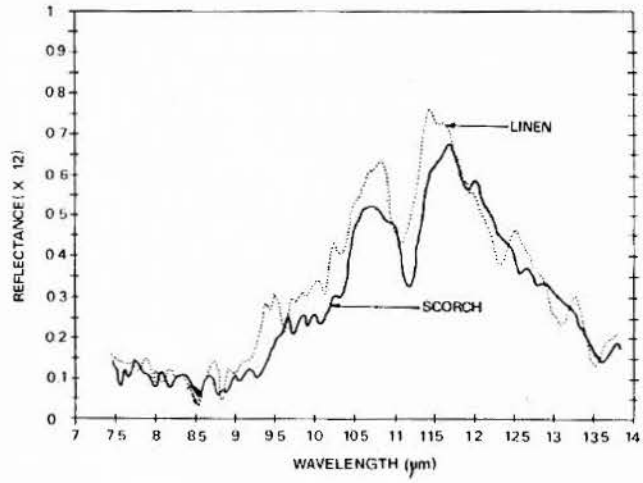

Fig. 7. Absolute spectral reflectance comparisons of linen and scorched linen in 8–14-μm band.

as measured with a moderate resolution laboratory instrument. Solid body spectra of common materials are generally broad featured,[4] and the spectral resolution so obtained was adjudged adequate for the expected spectral characteristics of the actual measurement.

D. Experimental Procedure

The focused blackbody source located ~40 cm from the target was positioned upon a preselected area of interest. The radiometer located ~2 m from the cloth was focused on the area and adjusted for maximum signal return. The narrow FOV of the instrument contributed to positioning sensitivity. However, once positioned, the signal levels were stable. A spectrum was recorded. The reference standard was then positioned directly over the area of interest, maintaining geometry, and another spectrum was recorded. Signal levels in the 3–5-μm band were considerably greater than in the 8–14-μm band, and corresponding attenuator changes were required.

Of particular note during the course of the experiment was the relatively large fluctuations in atmospheric absorption, especially on those days when local precipitation caused high relative humidity. Although sufficient data were taken to enable approximate spectral recovery, the atmospheric fluctuations from measurement to measurement accompanied by inherent system noise were of such amplitude that the determination of absolute values of reflectance was unreliable. A further difficulty with the circular variable filter on the radiometer necessitated termination prior to completion, resulting in fewer measurements than anticipated.

E. Data Reduction and Presentation

As previously discussed, data reduction was attempted in accordance with Eq. (4). In practice, difficulties arise, especially with spectra containing relatively narrowbanded features. It is obvious that if a certain spectral feature appears in both the sample and reference measurement, the ratio of these spectra in the region of the feature yields a constant; however, if a small shift in wavelength occurs in either measurement, an artifact is produced. The effect is similar if, for example, the atmospheric absorption changes between sample and standard measurements. These effects can be a source of considerable error in spectral measurements and adequately justify dual beam instrumental techniques.

Approximately fifty spectra were taken in the course of the experiment. Areas of interest were categorized as image, blood, scorch, and linen.

The image areas are those parts of the cloth containing the anatomical attributes of the figure in the cloth. Generally, spectra were taken in those areas where the image was visually dense.

The blood areas are those regions containing a light crimson stain resembling a common bloodstain to some degree but devoid of its characteristic reddish-brown coloring.

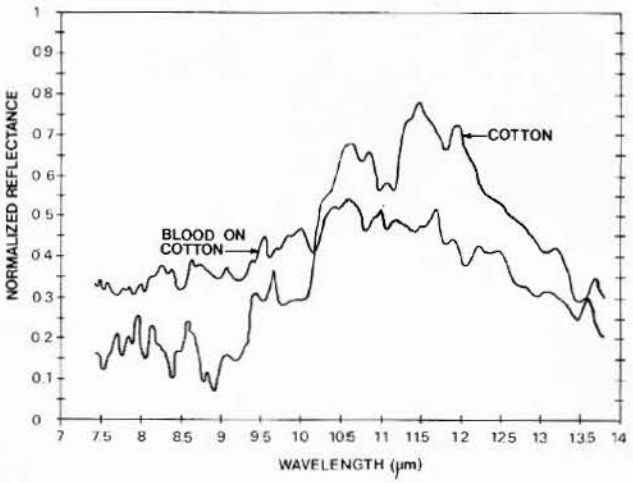

Fig. 8. Absolute spectral reflectance comparisons of cotton and whole blood-on-cotton in 8–14-μm band.

Linen refers to those regions containing no visual features and represents samplings of the background or homogeneous base layer of the cloth.

F. Discussion

Atmospheric fluctuations and noise precluded the data from being reduced in accordance with Eq. (4). As an alternative, a corrective spectral distribution was determined by forcing the normalized spectra of the featureless linen of the Shroud to agree with laboratory data on linen and then applying the calculated correction factor to the remaining measurements after normalization. This method allows spectral comparisons within the above approximation, but the absolute magnitude of the reflectance is lost.

As a point of reference several laboratory reflectance spectra are shown in Figs. 3–8. The spectral similarities of the samples are quite apparent. This result is largely true in both spectral bands with the exception of whole-blood-on-cotton in the 8–14-μm band. These results suggest that surface effects clearly dominate over known chemical differences in this region of the spectrum. From the data, the following observations are noted: Linen and cotton are spectrally similar in the 3–5- and 8–14-μm bands, both exhibiting pronounced features at 4.7 and 11 μm as shown in Figs. 3 and 6. In Fig. 3 a Sadtler KBr standard absorption spectrum is shown in comparison with a reflectance measurement. The pronounced feature at 3.5 μm appears subdued in the cotton reflectance spectrum and is absent in the linen spectrum. The feature that is present at 4.7 μm in reflectance is nearly absent in absorption. In general, caution is required in spectral comparisons between conventional absorption spectra and reflectance spectra because of the additional complications of refractive effects.

Spectral comparisons of linen and a moderate scorch shown in Fig. 4 display similar features in the 3–5- and 8–14-μm bands as shown in Fig. 7. In general, scorch

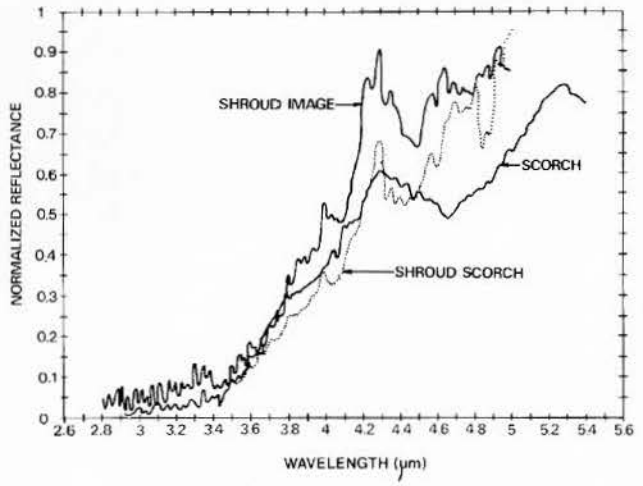

Fig. 9. Normalized spectral reflectance comparisons of scorched linen with averaged Shroud image and scorch areas in 3–5-μm band.

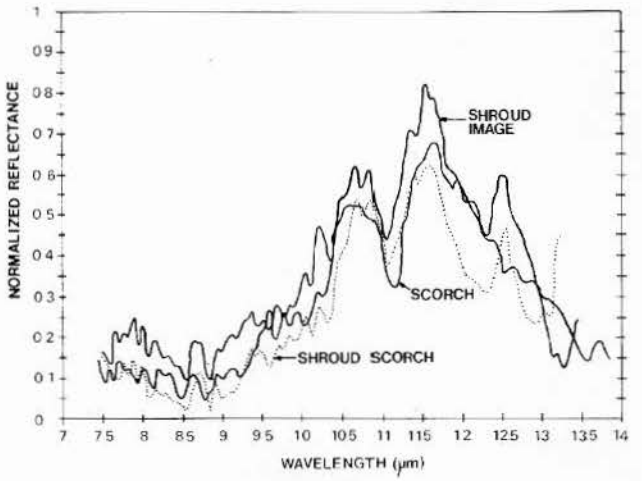

Fig. 10. Normalized spectral reflectance comparisons of scorched linen with averaged Shroud image and scorch areas in 8–14-μm band.

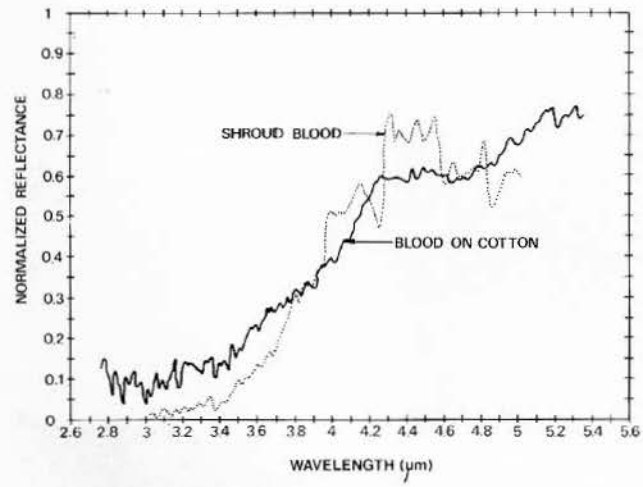

Fig. 11. Normalized spectral reflectance comparisons of blood-on-cotton with Shroud averaged blood areas in 3–5-μm band.

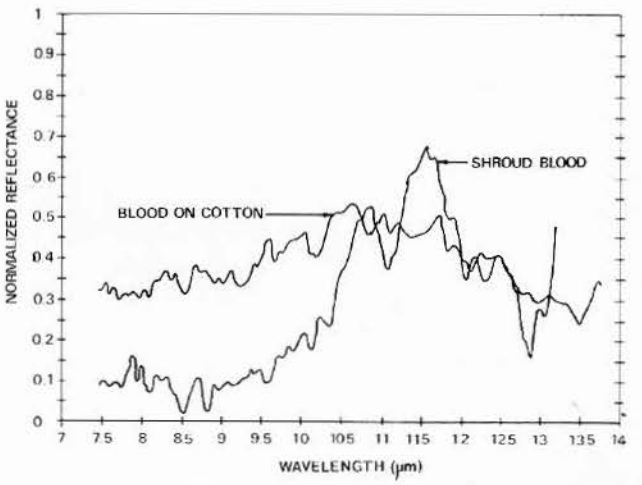

Fig. 12. Normalized spectral reflectance comparisons of whole blood-on-cotton with averaged Shroud blood in 8–14-μm band.

spectra are invariant with respect to visual intensity, showing nearly identical absolute reflectances in both spectral bands. Furthermore, there exists almost negligible spectral variation between scorches and bare linen. Blood-on-cotton in Fig. 5 has little effect on cotton spectral features in the 3–5-μm band but a pronounced effect in the 8–14-μm band as shown in Fig. 8.

Intercomparison between laboratory data and measurements on the Shroud yielded the following observations: As shown in Figs. 9 and 10, laboratory observations of scorches on linen are similar to scorches on the Shroud. Also shown is a marked similarity between image and scorch areas in both spectral bands. Blood comparisons show marked differences in both bands, the disparity in the 8–14-μm band being quite pronounced as shown in Figs. 11 and 12. A whole-blood-on-linen laboratory measurement was not available. However, since the base material spectra of cotton and linen were quite similar, it was reasoned that comparisons between blood-on-cotton and blood-on-linen were valid. These results are mitigated somewhat by the presumed age of the blood and by the possibility of its having undergone a rather large temperature excursion due to the fire. The effects of these factors on spectral features are unknown.

G. Conclusions

Due to the uncertainties in the data it is not possible to draw definitive conclusions. The spectral similarity of the image areas to known scorches is noted and is consistent with observation in terms of color in the visible region of the spectrum, however; this result is not without ambiguity since spectral similarities are characteristic of most areas examined as shown by the data in both spectral bands. Shroud blood comparisons with

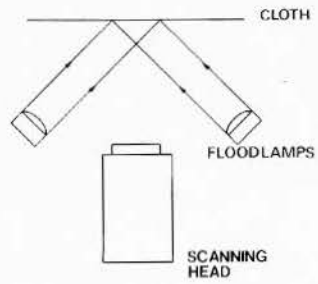

Fig. 13. Experimental configuration for IR imaging experiments.

known bloodstains show marked differences. It is not known if these differences are chemical or surface effects. With regard to the experiment in general, the many spectral similarities suggest that surface effects dominate over chemistry or composition in this region of the spectrum and that if chemical differences discernible by spectroscopic techniques in these spectral bands exist, they lie well below the limits of sensitivity of the instrumentation described herein. Without drastic improvements in instrumentation, a second attempt is not recommended.

III. Thermographic Investigations

Largely nonquantitative in this application, this technique was employed to observe inhomogeneities in the image attributable to differences in IR emissivities not otherwise detectable in the visible region. In addition to imaging in the IR spectral bands, it provides the additional advantage of observations over a fairly wide FOV.

Consider a generalized IR detector in a uniform environment at a constant temperature T_e and a body under observation at temperature T_b. We seek the change in equivalent temperature that results from a given change in emissivity. The total flux incident on the receiver can be written as

$$E = A\sigma\epsilon_B T_b^4 + B(1-\epsilon_B)\sigma T_e^4, \tag{5}$$

where σ = constant;
ϵ_b = total emissivity of body; and
A,B = factors associated with geometry.

The first term in the expression represents the self-emission term of the body and the second, the reflected background radiation. Differentiation with respect to T_b and ϵ_b yields

$$\frac{\partial E}{\partial T_b} = 4A\sigma\epsilon_B T_b^3, \qquad \frac{\partial E}{\partial \epsilon_b} = A\sigma T_b^4 - B\sigma T_e^4.$$

We demand the condition

$$\Delta E = \frac{\partial E}{\partial T_b}\Delta T_B = \frac{\partial E}{\partial \epsilon_b}\Delta\epsilon_b.$$

It follows that

$$\frac{\Delta T_b}{T_b} = \frac{\Delta\epsilon_b}{4\epsilon_b}\left(1 - \frac{BT_e^4}{AT_b^4}\right), \tag{6}$$

yielding the equivalent change in temperature due to a relative change in emissivity. It is clear that for large differences in T_b and T_e, the sensitivity to a change in emissivity is correspondingly increased.

If the temperature of a body is raised by illuminating with a source of radiation of intensity $I_0(\lambda)$, some of the radiation is thermalized, and the following equality is an expression of thermal equilibrium:

$$\int_0^\infty \alpha_b(\lambda) I_0(\lambda) d\lambda = \epsilon_b \sigma T_b^4, \tag{7}$$

where $\alpha_b(\lambda)$ = spectral absorptivity of the body.

If two such bodies are within the FOV, the flux difference or relative contrast may be written from Eq. (5) as

$$\Delta E = \sigma A(\epsilon_{b1} T_{b1}^4 - \epsilon_{b2} T_{b2}^4) - B\sigma T_e^4(\epsilon_{b1} - \epsilon_{b2}). \tag{8}$$

Substitution of Eq. (7) into Eq. (8) yields

$$\Delta E = \sigma A\left\{\int_0^\infty [\alpha_{b1}(\lambda) - \alpha_{b2}(\lambda)] I_0(\lambda) d\lambda\right\} - BT_e^4(\epsilon_{b1} - \epsilon_{b2}), \tag{9}$$

where the radiation contrast between two bodies is related to the spectral absorptivity. If $I_0(\lambda)$ is large, the second term containing the background effect can be dropped. Furthermore, if $I_0(\lambda)$ is limited to the visible portion of the spectrum and $\alpha(\lambda)$ is replaced by $1 - \rho(\lambda)$, where $\rho(\lambda)$ is the spectral reflectivity, Eq. (9) becomes

$$\Delta E = \sigma A \int_0^\infty [\rho_{b2}(\lambda) - \rho_{b1}(\lambda)] I_0(\lambda) d\lambda, \tag{10}$$

which is recognized as an expression describing contrast in the visible region of the spectrum between two bodies of spectral reflectivity $\rho_1(\lambda)$ and $\rho_2(\lambda)$. We conclude that the image observed in the IR region when illuminated with a source of strong visible radiation is approximately the image observed in the visible region with reversed contrast. We show in the following section that this result is experimentally verified within the limits of instrument resolution.

A. Experiment

Figure 13 depicts the experimental configuration. Imaging was accomplished in the 3–5- and 8–14-μm bands with thermographic scanning cameras. The source of illumination was two 1500-W photographic

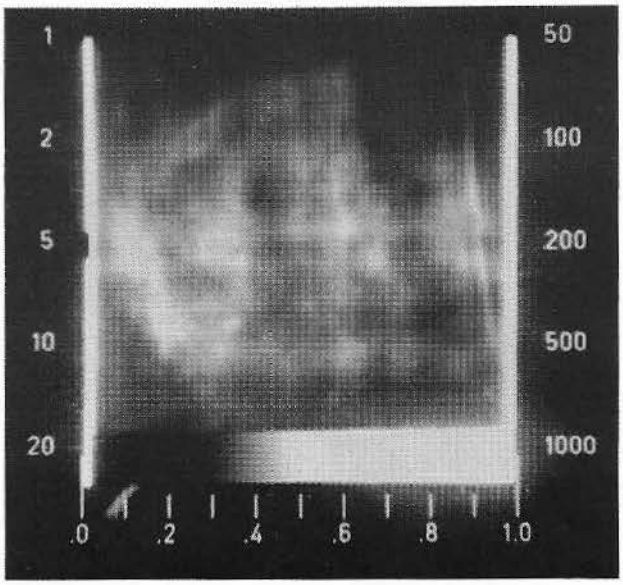

Fig. 14. Face region in 8–14-μm band. Features observed correspond closely to those observed in the visible with reversed contrast.

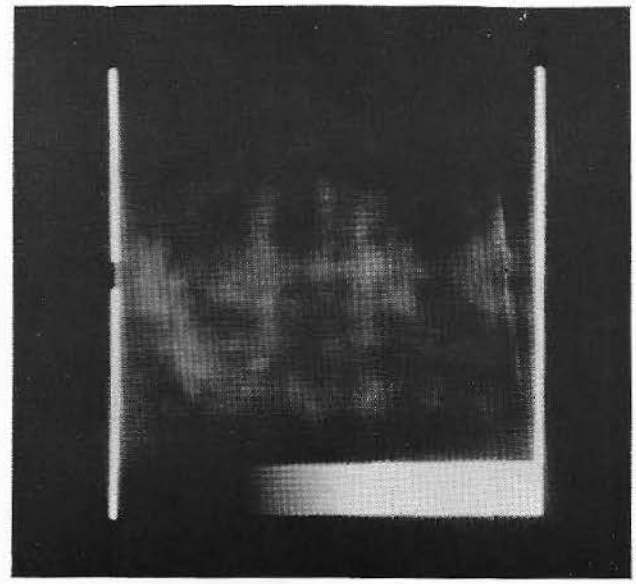

Fig. 15. As in Fig. 14 with slightly less contrast and scale lights turned off.

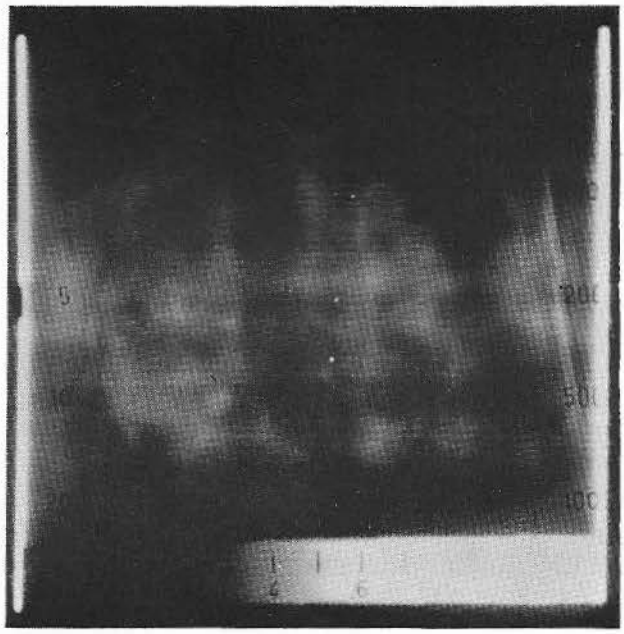

Fig. 16. As in Fig. 15 with image expansion.

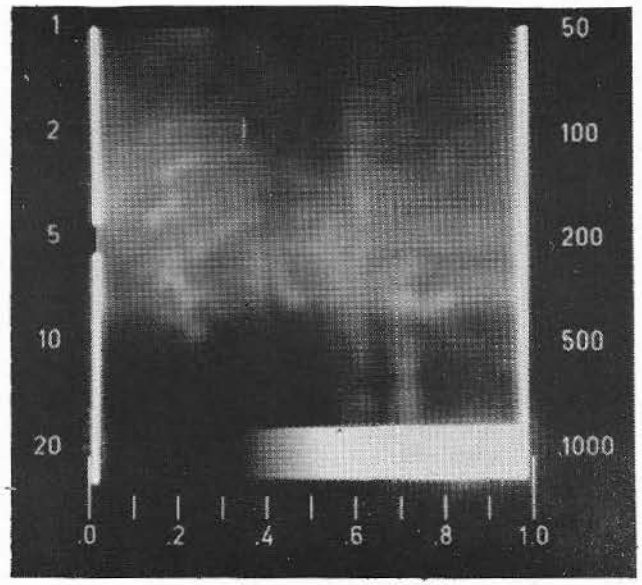

Fig. 17. Back of head in 8–14-μm band. Irregularly shaped brighter areas in upper part of photo correspond to red crimson stains in visible.

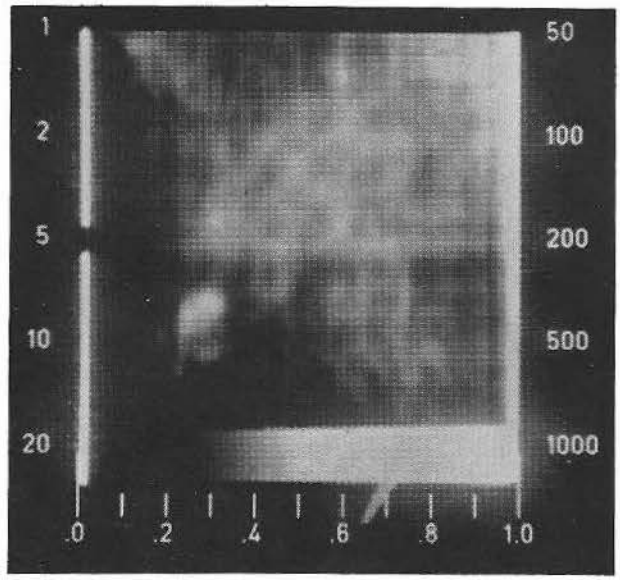

Fig. 18. Hands in 8–14-μm band. Bright spot in upper left of photograph corresponds to red crimson stain on wrist in visible.

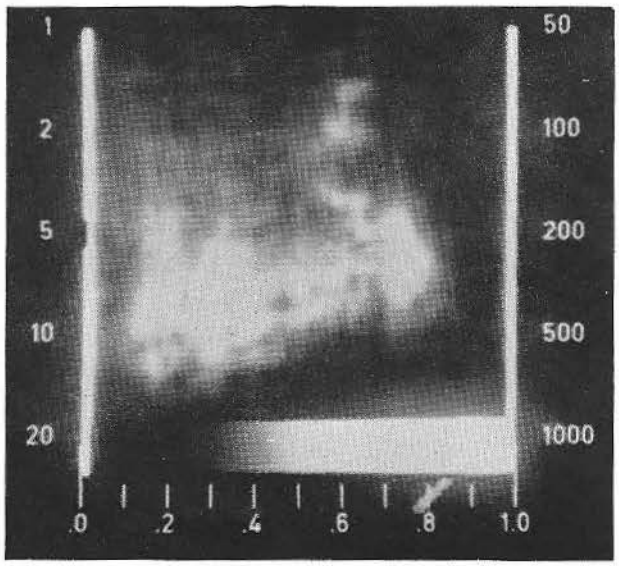

Fig. 19. Foot area in 8–14-μm band.

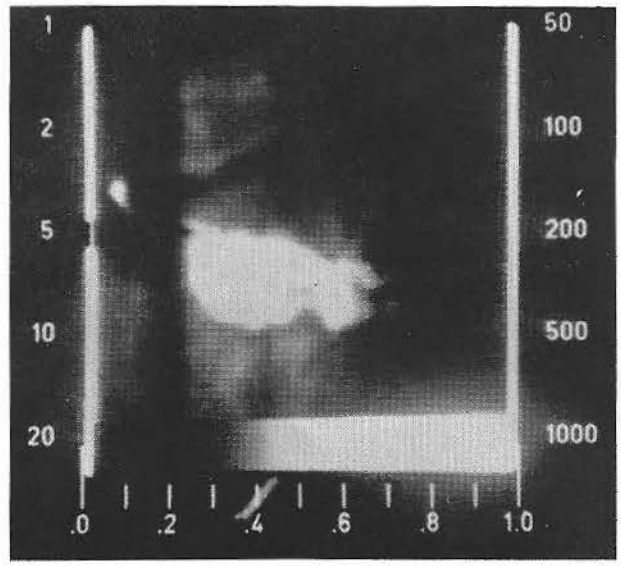

Fig. 20. Chest wound in 8–14-μm band. Bright patch corresponds to large crimson stain in visible. Irregular darker area corresponds to cloth patch sewn over a burned region from 1532 fire.

floodlamps, which when focused provided approximately uniform levels of illumination across the observed region. No contrast was discernible without the floodlamp illumination indicating that the emissivity differences in various features on the Shroud were below the limit of sensitivity of the cameras at room temperature. With illumination considerable contrast was noted in the 8–14-μm band as shown in Figs. 14–20. A nominal temperature span from black to white levels was 1.75°C. No features were observed in the 3–5-μm band regardless of illumination. This result is attributed to differences in instrument apertures and hence basic sensitivities rather than physical attributes of the surface. By observing the reflected arc lamp illumination from a gold-plated diffuse standard it was ascertained that no detectable radiation in the 8–14-μm

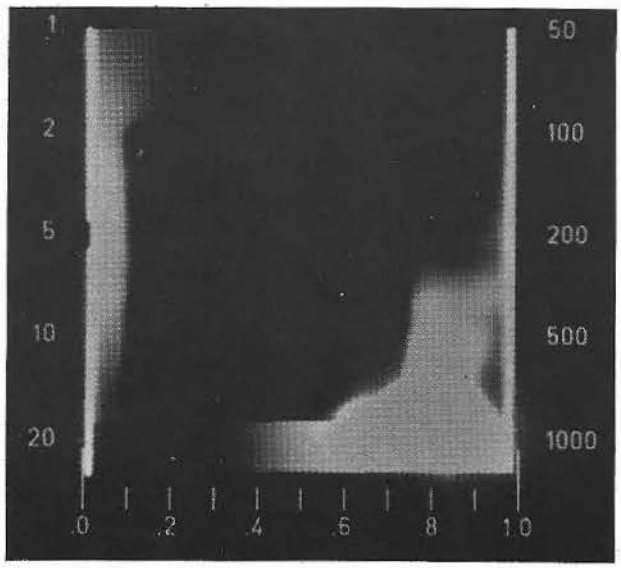

Fig. 21. Gold reflectance standard illuminated with floodlamps. Black level indicative of no detectable 8–14-μm radiation from floodlamps.

band was given off by the lamps. As shown in Fig. 21 the standard appears totally black with nominal control settings. Regions observed included the face, side wound, back of head, hands, and feet with contrast polarity such that the warmer features appear brighter.

B. Discussion

The lack of contrast with no illumination is attributed to a combination of $(\Delta\epsilon)/\epsilon \ll 1$ and $T_e \simeq T_b$ [referenced to Eq. (6)] necessitating an increase in target temperature in excess of the background temperature to attain acceptable contrast levels. This results in similar features showing negligible differences in absolute reflectivities. The general character of the illuminated imagery reflects the validity of Eq. (10) in that it appears much like a black-and-white negative print. It is noted that the featureless linen background appears black in the IR rendition. The crimson stains evident on plates of the side wound, hands, face, and feet appear relatively bright as opposed to the visible appearance. Scorch and image areas lie intermediate between the two. The IR imagery is a reversed approximate replica of the image observed in the visible region with no inhomogeneities or artifact apparent to the authors. Since the inherent resolution of the IR camera is poorer than the high quality photographic imagery, this result can be questioned, however; if such an artifact exists, it lies below the limit of resolution obtainable with this instrumentation.

C. Conclusions

We have shown that emissivity differences in various features of the Shroud are too small to yield recognizable images in the 3–5- or 8–14-μm band with instruments of temperature sensitivity on the order of $\Delta T \simeq 0.5$°C or less. This result is consistent with comparisons of laboratory reflectance values of similar materials. With artificial uniform visible illumination good imagery was observed in the 8–14-μm band, however; this illumination scheme yields an image closely correlated to the image obtained in the visible region with reversed contrast. This result is consistent with theoretical considerations. With due regard to the limits of instrument resolution and sensitivity, it is the authors' opinion that no significant anomalies exist; however, we leave the final interpretation to those competent in these matters.

The authors wish to thank P. Rinaldi, A. Otterbein, and L. Gonella for their efforts in making this project possible. We gratefully acknowledge the invaluable advice and assistance from our many fellow investigators on this project and to those individuals and corporations whose financial contributions provided sorely needed support.

This work was sponsored by Shroud of Turin Research Project, Inc. It was substantially accomplished when both authors were with U.S. Air Force Weapons Laboratory, Albuquerque, New Mexico. Affiliation with the authors's present employers is coincidental, and no sponsorship or endorsement is implied.

References

1. E. J. Jumper and R. W. Mettern, Appl. Opt. **19**, 1909 (1980).
2. For a rather vague reference to possible parallels see *Encyclopedia Britannica* (U. Chicago, 1979), Vol. 14, p. 1085.
3. N. L. Alpert, W. E. Keiser, and H. A. Symanski, *IR: Theory and Practice of Infrared Spectroscopy* (Plenum, New York, 1970), pp. 7, 8.
4. W. Wolfe, U. Arizona; private communication.
5. W. Wolfe and G. Zissis, *The Infrared Handbook* (Environmental Research Institute of Michigan, Ann Arbor, 1978), pp. 3-84–3-154.
6. S. Pellicori, Appl. Opt. this issue **19**, 1913 (1980).